The effects of shear on Mode II delamination: a critical review

Paolo S. Valvo
Department of Civil and Industrial Engineering, University of Pisa, Italy
p.valvo@ing.unipi.it, http://orcid.org/0000-0001-6439-1926

ABSTRACT. The paper focuses on the effects of shear deformation and shear forces on the mode II contribution to the energy release rate in delaminated beams. A critical review of the relevant literature is presented, starting from the end-notched flexure test as the prototype of delaminated laminates subjected to pure mode II fracture. Several models of the literature are recalled from simple beam theory to more refined models. The role of first-order shear deformation in line with the Timoshenko beam theory is investigated as distinct from the local crack-tip deformation related to the shear modulus of the material. Then, attention is moved on to a general delaminated beam with an arbitrarily located through-the-width delamination, subjected to mixed-mode fracture. Several fracture mode partition methods of the literature are reviewed with specific attention on the effects of shear on the mode II contribution to the energy release rate.

KEYWORDS. Delamination; Mixed-mode fracture; Mode II fracture; Beam theory; Shear deformation; End-notched flexure test.

Citation: Valvo, P.S., The effects of shear on Mode II delamination: a critical review, Frattura ed Integrità Strutturale, 44 (2018) 123-139.

Received: 10.02.2018
Accepted: 23.02.2018
Published: 01.04.2018

INTRODUCTION

Delamination, or interlaminar fracture, is a major failure mode for composite laminates, which still attracts researchers' attention despite the huge number of dedicated studies during the last decades [1–5]. Since the earlier works, it has been recognised that the structural behaviour of a laminate affected by delamination can be analysed by schematising the laminate as an appropriate assemblage of sublaminates [6, 7]. These are in turn modelled as plates or beams, depending on the geometry, loads, and boundary conditions of the particular problem at hand. Proper homogenisation techniques are used to obtain the overall laminate stiffnesses [8].

The Euler-Bernoulli beam theory – also referred to in the literature as classical or simple beam theory (SBT) – is the most elementary structural theory that can be used in this context. SBT assumes that the plane cross sections of a beam remain plane and orthogonal to the centreline after deformation. Thus, SBT completely neglects shear deformation, which indeed can be relevant for composite laminates because of the orthotropic material behaviour. Shear deformation is taken into account at first order by the Timoshenko beam theory (TBT), which admits relative rotations between the plane cross sections and the centreline of a beam [9]. Simple and Timoshenko beam theories correspond to the Kirchhoff-Love and Mindlin-Reissner theories for thin and thick plates, respectively [10]. Higher-order shear-deformation theories (HSDT) for

beams and plates assume that plane cross sections may not remain plane, which enables better agreement between the structural models and three-dimensional elastic analyses. After the pioneering work by Reddy [11], several modified HSDTs have been developed (see Ref. [12] for a recent review), including specialised versions for the analysis of delaminated plates [13, 14].

Besides the adoption of a more or less refined structural theory for the sublaminates, the connection between them has to be suitably described. To this aim, models of growing complexity can be chosen, ranging from rigid connections [15–24] to elastic interfaces [25–38] and cohesive zone models [39–47]. This choice is relevant not only for the accurate prediction of the laminate structural response – e.g. in terms of displacements, stresses, etc. – but also for the evaluation of crack growth. In fact, the type of connection model determines the type of description of the stress field at the delamination crack front. With a rigid connection, the stress field will be represented by concentrated forces and couples, whereas with deformable interfaces there will be a distribution of peeling and shearing stresses [23]. Based on such quantities, typical fracture mechanics parameters can be evaluated. Within linear elastic fracture mechanics (LEFM), the energy release rate, G, is commonly considered to predict the initiation and growth of delamination cracks [48]. However, delamination cracks usually propagate under a mix of the three basic fracture modes (I or opening, II or sliding, and III or tearing). Therefore, appropriate mixed-mode partition methods are adopted to decompose G into the sum of three modal contributions, G_{I}, G_{II}, and G_{III} [49]. Besides, suitable experimental procedures are used to characterise the delamination toughness in pure and mixed fracture mode conditions [50]. In particular, for pure mode II, the end-notched flexure (ENF) test is the current standard [51].

This paper focuses on delaminated laminates modelled according to simple or Timoshenko beam theories with rigid connections or elastic interfaces. The aim is to shed light on the effects of shear deformation and shear forces on the mode II contribution, G_{II}, to the energy release rate. Literature on this topic is contradictory with some Authors asserting [19, 21, 31, 46] and others negating [16, 20, 24, 30, 36] this effect. As will be illustrated, the origin of this controversy can be dated back to a series of papers on the analysis of the ENF test [52–65]. In particular, Carlsson et al. [53] modelled the ENF test by using the Timoshenko beam theory and found correction terms depending on shear deformation for both the specimen compliance, C, and energy release rate, G_{II}. Their formulas have been widely used in the later literature for the interpretation of experimental results [66–68] and comparison purposes [69–71]. Unfortunately, as pointed out by Fan et al. [64], the derivation of such formulas was biased by a wrong boundary condition. Actually, Silva et al. [63] had obtained the correct expressions for C and G_{II} according to the TBT: the compliance does have a term depending on shear deformation, which however does not depend on the crack length, a. Hence, this term vanishes when differentiating C with respect to a to obtain G_{II} according to the well-know Irwin–Kies formula [72]. Notwithstanding the above, the wrong formulas from [53] are still used even in the more recent literature [73–77] and reported in the latest edition of an otherwise excellent book [50].

This paper extends some preliminary considerations by the Author [75], also in the light of new findings in the recent literature. The outline is as follows. First, a review on the analysis of the ENF test is given and some preliminary conclusions are drawn for laminates with symmetric – i.e. placed on the mid-plane – delamination. Then, attention is moved on to a general delaminated beam with a through-the-width delamination arbitrarily located in the thickness. In this case, mixed-mode fracture conditions generally occur with $G = G_{\mathrm{I}} + G_{\mathrm{II}}$. Several mixed-mode partition methods of the literature are reviewed with specific attention on the effects of shear forces and shear deformation on G_{II}. Lastly, a quantitative comparison is pursued between the predictions for G_{I} and G_{II} stemming from (i) a rigid-connection model [24], (ii) an elastic-interface model [37], and (iii) a solution based on the theory of elasticity [21].

END-NOTCHED FLEXURE TEST

The end-notched flexure (ENF) test has been recently standardised by ASTM International as the method for the characterisation of mode II delamination toughness of unidirectional fibre-reinforced composite laminates [51]. In the test, a laminated specimen with rectangular cross section is loaded by a force P in a three-point bending configuration. Let $L = 2l$ denote the specimen length, B and $H = 2h$ the cross-section width and thickness, respectively. Specimens are prepared with a mid-plane delamination crack at one of their ends. Let a be the delamination length. A Cartesian reference system $Oxyz$ is fixed with the origin O at the centre of the crack-tip cross section, the x-axis aligned with the specimen's longitudinal direction, the z-axis pointing downwards, and the y-axis completing the right-handed reference frame (Fig. 1).

The ENF test specimen can be considered as subject to an antisymmetric loading condition with respect to its mid-plane (Fig. 2). In this case, if also material properties have a symmetric distribution with respect to the mid-plane, then normal stresses on the delamination plane will be null. Hence, pure mode II fracture conditions will be attained. This is the case of

homogeneous and orthotropic specimens, as well as unidirectional laminated specimens and multidirectional laminated specimens with symmetric lay-ups. It is hardly necessary to remember that in the asymmetric end-notched flexure (AENF) test, the delamination crack will generally be subjected to mixed-mode fracture conditions [79–82]. In the following, focus will be on a homogeneous and orthotropic specimen. The elasticity moduli in the material reference will be denoted as E_x, E_z, G_{xz}, and ν_{xz} [8].

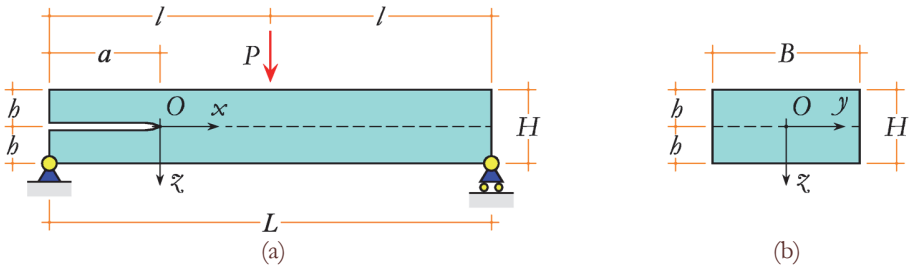

Figure 1: Scheme of the end-notched flexure (ENF) test: (a) side view; (b) cross section.

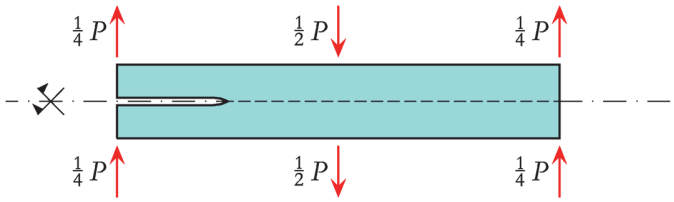

Figure 2: Free-body diagram of the ENF test specimen.

For the following analysis, it is useful to introduce the specimen compliance,

$$C = \frac{\delta}{P} \tag{1}$$

defined as the ratio between the displacement, δ, of the load application poin and the load intensity, P. Furthermore, the energy release rate, G, is defined as the decrease of potential energy of the system spent in the crack growth process, per unit area of new surface created. The energy release rate can be obtained by differentiating the compliance with respect to delamination length according to the Irwin–Kies formula [72]:

$$G = \frac{P^2}{2B}\frac{dC}{da} \tag{2}$$

Depending on the adopted structural model, various expressions for the specimen compliance have been obtained in the literature. Correspondingly, various expressions for the energy release rate are deduced through Eq. (2).

Simple and Timoshenko beam-theory models

The ENF test was first used for composite materials by Russell and Street [52], who applied simple beam theory (SBT) to determine the specimen compliance,

$$C_{\mathrm{ENF}}^{\mathrm{SBT}} = \frac{2l^3 + 3a^3}{8E_x B h^3} \tag{3}$$

and energy release rate,

$$G_{\mathrm{ENF}}^{\mathrm{SBT}} = \frac{9P^2 a^2}{16E_x B^2 h^3} \tag{4}$$

To consider shear deformation, Carlsson et al. [53] modelled the ENF test via the Timoshenko beam theory (TBT) [9] and obtained the following expressions:

$$C_{\mathrm{ENF}}^{\mathrm{Carlsson,Gillespie,Pipes}} = \frac{2l^3+3a^3}{8E_x Bh^3}\left(1+2\frac{E_x}{G_{xz}}\frac{1.2l+0.9a}{2l^3+3a^3}h^2\right) \tag{5}$$

for the compliance, and

$$G_{\mathrm{ENF}}^{\mathrm{Carlsson,Gillespie,Pipes}} = \frac{9P^2a^2}{16E_x B^2h^3}\left[1+\frac{2}{10}\frac{E_x}{G_{xz}}\left(\frac{h}{a}\right)^2\right] \tag{6}$$

for the energy release rate. However, Whitney [55] promptly observed that «continuity of displacement at the crack tip is not attained with the approach that yields» Eqs. (5) and (6). Later, also Fan et al. [64] realised that «a false assumption was made in the derivation», leading to «inconsistency (…) for the expressions that are used to calculate the energy release rate». Actually, in Ref. [53] the cross-section rotation at the crack tip is taken equal to the slope of the deflected beam, but this assumption manifestly contradicts the hypotheses on which Timoshenko's first-order shear-deformation beam theory is based. As a matter of fact, by applying the TBT without the above unnecessary approximations, Silva et al. [63] obtained:

$$C_{\mathrm{ENF}}^{\mathrm{TBT}} = \frac{2l^3+3a^3}{8E_x Bh^3}+\frac{3l}{10G_{xz}Bh} = C_{\mathrm{ENF}}^{\mathrm{SBT}}+\frac{3l}{10G_{xz}Bh} \tag{7}$$

for the compliance, and

$$G_{\mathrm{ENF}}^{\mathrm{TBT}} = \frac{9P^2a^2}{16E_x B^2h^3} = G_{\mathrm{ENF}}^{\mathrm{SBT}} \tag{8}$$

for the energy release rate. Eq. (7) shows that shear deformation at first order modifies the compliance with an additional term with respect to simple beam theory. This correction terms is however constant with respect to a, hence it vanishes when applying Eq. (2) to deduce the energy release rate. Thus, as Eq. (8) shows, G_{II} turns out to have the same expression according to both SBT and TBT. To confirm this, it is instructive to examine qualitatively the deformed shapes due to shear only of two ENF test specimens with shorter (Fig. 3a) and longer (Fig. 3b) delamination cracks. If the specimen is modelled as an assemblage of rigidly connected sublaminates, the deformed shape due to shear is clearly independent of the delamination length, a.

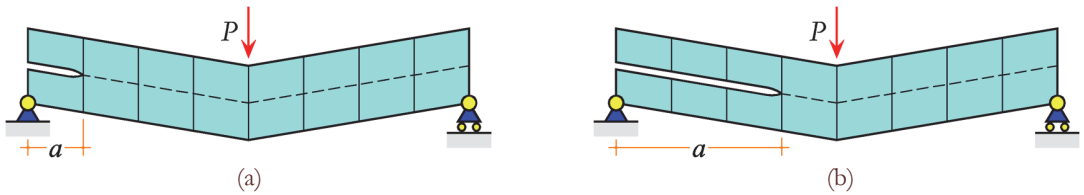

Figure 3: Rigid-connection model of the ENF test: deformed shapes due to shear for (a) shorter and (b) longer delamination cracks.

In this respect, it can be mentioned that Ozdil et al. [59] analysed the ENF test using shear-deformation laminated plate theory and found that «there is no (…) contribution from shear deformation to the energy release rate for unidirectional (…) laminates with mid-plane cracks», while a «very small contribution» emerges for angle-ply laminates. Also, Chatterjee [56] used shear-deformation laminated plate theory to study the ENF test and found that «the energy release rate (…) will not be affected if shear deformation effects (in the context of beam theory) are neglected».

Elasticity-theory models

Authors who modelled the ENF test within the theory of elasticity generally obtained numerical results showing a dependence of the energy release rate on the shear modulus of the material [54, 56, 57].

Chatterjee [56] suggested the following semi-empirical expression to match the elasticity theory solution:

$$G_{\mathrm{ENF}}^{\mathrm{Chatterjee}} = \frac{9P^2a^2}{16E_x B^2 h^3}\left(1+0.13\sqrt{\frac{E_x}{G_{xz}}}\frac{h}{a}\right)^2 \tag{9}$$

Wang and Williams [57] used finite element analysis and found a dependence of both the compliance and energy release rate on the shear modulus of the material. They observed that their numerical results for the energy release rate could be approximated by introducing an increased delamination length into the SBT expression, Eq. (4):

$$G_{\mathrm{ENF}}^{\mathrm{Williams}} = \frac{9P^2(a+\chi h)^2}{16E_x B^2 h^3}, \quad \text{where} \quad \chi = \sqrt{\frac{1}{63}\frac{E_x}{G_{xz}}\left[3-2\left(\frac{\Gamma}{1+\Gamma}\right)^2\right]} \quad \text{and} \quad \Gamma = 1.18\frac{\sqrt{E_x E_z}}{G_{xz}} \tag{10}$$

A similar crack-length correction parameter, χ, was later adopted by many Authors [36, 62]. Today, it is also suggested in the standard method for the mixed-mode bending (MMB) test [83].
Andrews and Massabò [21], based on finite element analyses, gave the following expression for the energy release rate of an orthotropic ENF test specimen:

$$G_{\mathrm{ENF}}^{\mathrm{Andrews,Massabò}} = \frac{9P^2a^2}{16E_x B^2 h^3}\left[1-\frac{1}{12}\left(a_1^N + a_2^N\right)\frac{h}{a} - \frac{2}{9}\left(a_1^{Vs} + a_2^{Vs}\right)\left(\frac{h}{a}\right)^2\right] \tag{11}$$

where a_1^N, a_2^N, a_1^{Vs}, and a_2^{Vs} are compliance coefficients given in a tabular form as functions of the material elastic moduli, including the shear modulus. Andrews and Massabò's solution [21] highlights the fact that local deformation – in particular, deformation related to root rotations, i.e. the rotations of the sublaminate cross sections at the crack tip – plays a relevant role in delamination fracture problems. It is also noteworthy that for isotropic materials, Eq. (11) degenerates into Eq. (9).

Higher-order shear-deformation theory models

Whitney [55] used second-order shear-deformation beam theory (SOBT) and obtained the following approximate polynomial solution for the energy release rate:

$$G_{\mathrm{ENF}}^{\mathrm{Whitney}} = \frac{9P^2a^2}{16E_x B^2 h^3}\left[1+2\frac{h}{\lambda a}+\frac{131}{75}\left(\frac{h}{\lambda a}\right)^2\right], \quad \text{where} \quad \lambda = 4\sqrt{\frac{14}{5}\frac{G_{xz}}{E_x}} \tag{12}$$

Pavan Kumar and Raghu Prasad [61, 65] compared simple beam theory with first-order (i.e. TBT), second-order (SOBT), and third-order shear-deformation beam theories (TOBT). Through numerical computation, they found that the simple and Timoshenko beam theory models of the ENF test yield the same values of the energy release rate, while the higher-order beam theory models furnish larger values. For short crack lengths, they reported that the TOBT model gives corrections to G_{II} up to 30% of $G_{\mathrm{ENF}}^{\mathrm{SBT}}$ for unidirectional laminated specimens and nearly 50% for multidirectional laminated specimens. They also found that TOBT was in good agreement with the results of finite element analyses.

Elastic-interface models

Corleto and Hogan [58] modelled the ENF test by considering the upper half laminate as a Timoshenko beam on a generalised elastic foundation consisting of extensional and rotational distributed springs. They found that the energy release rate is independent of the shear stiffness of the sublaminate, $5/6\, G_{xz}Bh$, but not of the shear modulus of the material, G_{xz}, which enters the expressions of the elastic constants of the foundation. Based on this result, Ding and Kortschot [60] used SBT to deduce a simplified model of the ENF test, where the foundation consists of tangential springs only.
Wang and Qiao [62] used TBT and considered an elastic foundation made of distributed tangential springs. By neglecting some numerically small terms in the solution, they obtained the following expression:

$$C_{\mathrm{ENF}}^{\mathrm{Wang,Qiao}} = \frac{3a^3 + 2l^3}{8E_x B h^3} + \frac{3l}{10G_{xz} B h} + \frac{9}{8E_x B}\chi\left[\left(\frac{a}{h}\right)^2 + \chi\frac{a}{h}\right] \tag{13}$$

for the compliance, and

$$G_{\mathrm{ENF}}^{\mathrm{Wang,Qiao}} = \frac{9P^2(a+\chi h)^2}{16E_x B^2 h^3}, \quad \text{where} \quad \chi = \sqrt{\frac{E_x}{12\lambda G_{xz}}} \quad \text{and} \quad \lambda \cong 5 \tag{14}$$

for the energy release rate. Eq. (13) shows that the shear stiffness influences the specimen's compliance, but not the energy release rate. The latter, however, is dependent on the shear modulus of the material through the crack-length correction parameter, χ.

A similar result was obtained by Bennati et al. [35, 36], who developed an enhanced beam-theory (EBT) model of the MMB test, where the sublaminates are flexible, extensible, and shear-deformable laminated beams, partly connected by an elastic interface consisting of normal and tangential springs. As a special case, they obtained the solution for an orthotropic ENF test specimen in terms of compliance,

$$C_{\mathrm{ENF}}^{\mathrm{EBT}} = \frac{3a^3 + 2l^3}{8E_x B h^3} + \frac{3l}{10G_{xz} B h} + \frac{9}{8E_x B}\chi\left[\left(\frac{a}{h}\right)^2 + \chi\left(\frac{a+2l}{h}\right) - 2\chi^2 - 4\chi\frac{a}{h}\exp\left(-\frac{l-a}{\chi h}\right)\right] \tag{15}$$

and energy release rate,

$$G_{\mathrm{ENF}}^{\mathrm{EBT}} = \frac{9P^2(a+\chi h)^2}{16E_x B^2 h^3}, \quad \text{where} \quad \chi = \sqrt{\frac{E_x}{8k_x h}} \tag{16}$$

The third addend in Eq. (15) comes from the deformability of the elastic interface. Eq. (15) differs slightly from Eq. (13), but furnishes quite similar numerical values. Also according to the EBT model, the shear deformability does not influence the mode II contribution to the energy release rate. However, it should be noted that, albeit the shear modulus, G_{xz}, does not enter explicitly Eq. (16), it is related to the elastic interface constant, k_x [27].

As for models with rigidly connected sublaminates, this result is perfectly intuitive for elastic-interface models if the deformed shapes of two specimens with different delamination lengths are considered (Fig. 4).

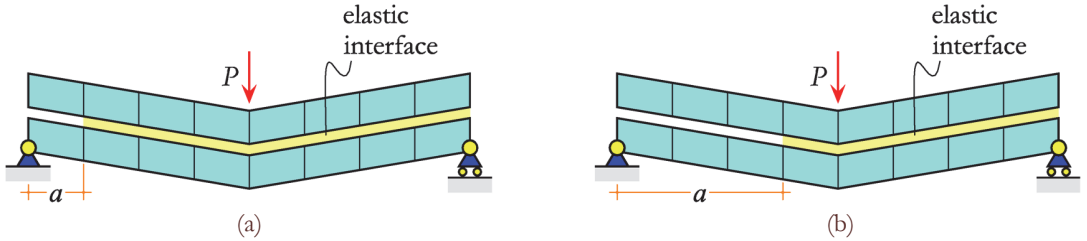

Figure 4: Elastic-interface model of the ENF test: deformed shapes due to shear for (a) shorter and (b) longer delamination cracks.

Preliminary conclusions

From the above literature review, the following preliminary conclusions can be drawn with reference to the ENF test:

- three-dimensional finite element analyses show that both the specimen compliance, C, and energy release rate, G_{II}, exhibit a dependence on the shear modulus of the material, G_{xz};
- the Timoshenko beam theory adds a correction term with respect to simple beam theory into the expression of C, depending on the (half) specimen shear stiffness, $5/6\ G_{xz}Bh$;
- the above correction term is constant with respect to delamination length, a; hence, it does not influence the energy release rate, G_{II}, which turns out to be independent of shear deformation at first order;
- some widely used expressions of the literature for C and G_{II} accounting for shear deformation turned out to be wrong;
- the dependence of G_{II} on G_{xz} seems to be related to local deformation occurring in the neighbourhood of the delamination front because of high stress concentration, e.g. strain in the laminate thickness direction, Poisson's effect, and root rotations;

- to catch such effects, it is necessary to use complex models, such as those based on the theory of elasticity or higher-order shear-deformation beam theories; alternatively, enhanced beam theory models with deformable – elastic or cohesive – interfaces between the delaminating sublaminates can be effectively used.

The above considerations can be extended from the ENF test to similar mode II delamination tests – e.g. the end-loaded split (ELS) test, the four-point end-notched flexure (4ENF) test, etc. [69] – where the specimen has a mid-plane delamination. In this case, fracture modes I and II are related to the symmetric and antisymmetric external forces acting on the specimen, respectively. Instead, the analysis of laminates with delamination cracks arbitrarily placed in the thickness requires the adoption of more complex mixed-mode partition methods. These will be the subject of the next section.

GENERAL DELAMINATED LAMINATES

Attention is now moved on to a general delaminated beam with an arbitrarily located through-the-width delamination. Let L be the laminate length, B and $H = 2h$ the cross-section width and height, respectively. A Cartesian reference system $Oxyz$ is fixed with the origin O at the geometric centre of one of the end sections, the x-axis aligned with the laminate longitudinal direction, the y- and z-axes aligned with the cross-section width and height directions, respectively (Fig. 5a). The analysis can be limited to an infinitesimal beam segment included between two cross sections located immediately behind and ahead of the delamination front. The delamination is not necessarily placed on the mid-plane, but divides the laminate into two sublaminates with thicknesses $H_1 = 2h_1$ and $H_2 = 2h_2$ (Fig. 5b) [24].

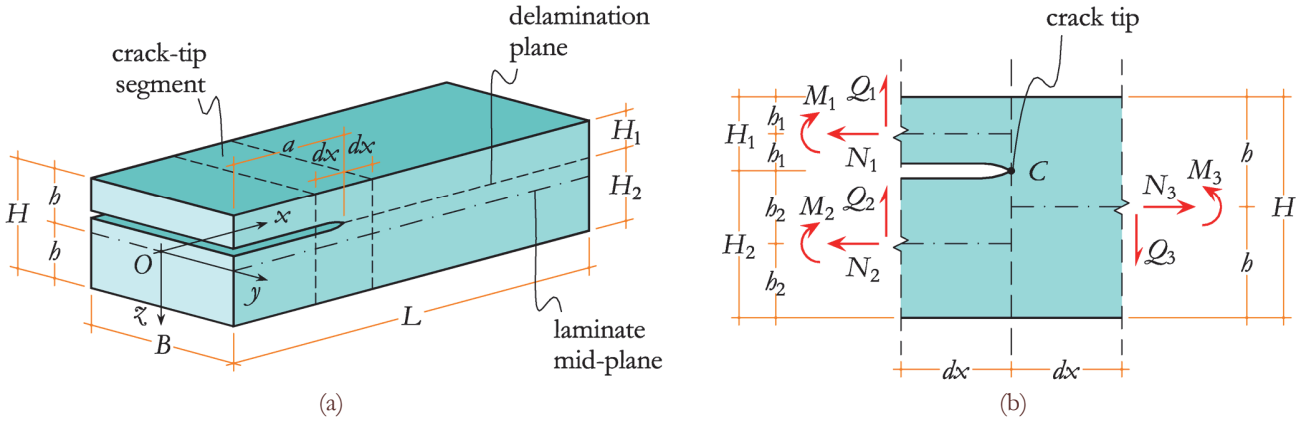

Figure 5: (a) General delaminated beam and (b) crack-tip segment.

Rigid-connection models

If the delaminated beam is modelled as an assemblage of rigidly connected sublaminates, the total energy release rate can be evaluated based on beam theory [21–24]. Thus, an analytical expression for G is determined depending on the values of the internal forces acting on the crack-tip segment: the axial forces, N_i, shear forces, Q_i, and bending moments, M_i ($i = 1, 2, 3$). However, to distinguish the single contributions stemming from fracture modes, G_I and G_II, it is necessary to introduce additional assumptions. To this aim, several fracture mode partition methods have been proposed in the literature. Williams' global method [16] is based on the analysis of the external forces globally acting on the laminate. The method assumes that fracture mode I is produced when opposite bending moments act on the two sublaminates into which the laminate is split; besides, mode II is obtained when the sublaminates have equal curvatures. As a consequence, the following expressions for the modal contributions to G can be obtained:

$$G_\mathrm{I}^\mathrm{Williams} = \frac{6}{E_x B^2}\frac{1}{H_2^3}\left[1+\left(\frac{H_2}{H_1}\right)^3\right]M_\mathrm{I}^2 + \frac{6}{10G_{zx}B^2}\left(\frac{1}{H_1}+\frac{1}{H_2}\right)Q_\mathrm{I}^2 \quad \text{and}$$
$$G_\mathrm{II}^\mathrm{Williams} = \frac{1}{2E_x B^2}\frac{H}{H_1 H_2}\left(1-2\frac{H_1}{H}\right)^2 N_\mathrm{II}^2 + \frac{18}{E_x B^2}\frac{H_2}{H_1^2}\left[1+\left(\frac{H_2}{H_1}\right)^3\right]M_\mathrm{II}^2, \tag{17}$$

where

$$N_{\mathrm{II}} = N_1 - \frac{\xi}{1-\xi} N_2, \quad Q_{\mathrm{I}} = \xi Q_2 - (1-\xi) Q_1, \quad M_{\mathrm{I}} = \frac{M_2 - \psi M_1}{1+\psi}, \quad \text{and} \quad M_{\mathrm{II}} = \frac{M_1 + M_2}{1+\psi} \tag{18}$$

with

$$\xi = \frac{H_1}{H} \quad \text{and} \quad \psi = \left(\frac{1}{\xi} - 1 \right)^3 = \left(\frac{H_2}{H_1} \right)^3 \tag{19}$$

According to Eqs. (17)–(19), axial forces produce only mode II, shear forces (and shear deformation) give only mode I, while bending moments contribute to both modes I and II.
Schapery and Davidson [18] observed that Williams' assumptions on the partition of fracture modes are not generally fulfilled if the delamination crack is not placed on the laminate mid-plane. Hence, they proposed a method based on classical laminated plate theory, where the mode I and II contributions to the energy release rate depend on the stress resultants – an axial force, N_C, and a bending moment, M_C – exchanged between the upper and lower sublaminates at the crack tip (Fig. 6a, b). Schapery and Davidson did not consider shear forces and shear deformation in their method.

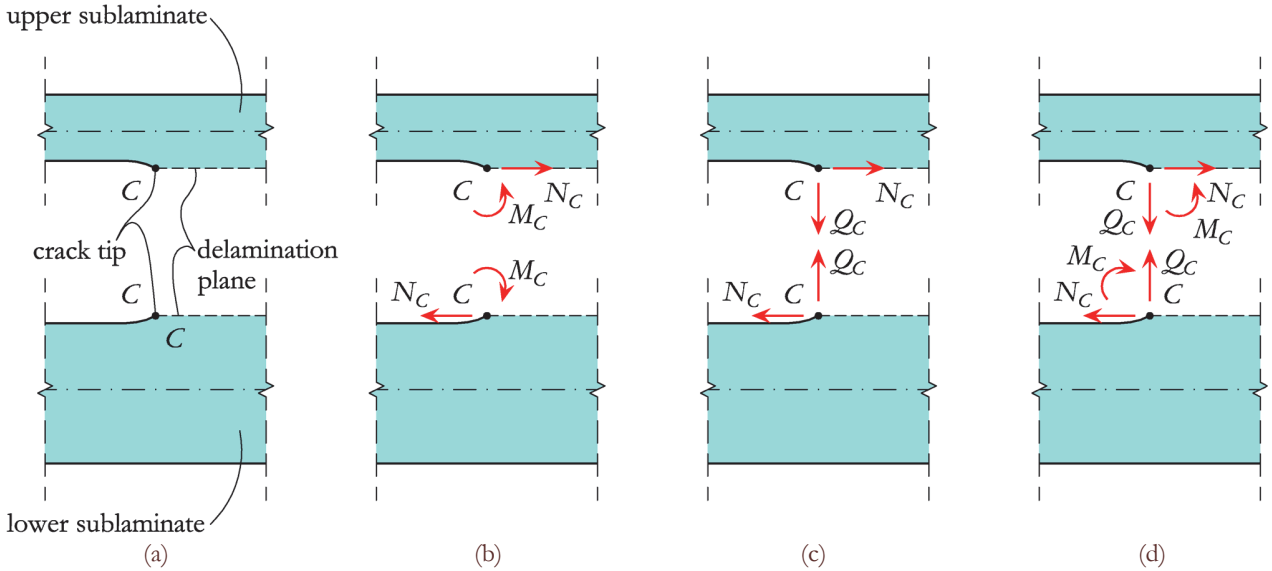

Figure 6: Crack-tip forces on (a) a split crack-tip segment, according to (b) Schapery and Davidson [18], (c) Wang and Qiao [20], and (d) Valvo [24].

Wang and Qiao [20] considered two perfectly bonded, shear-deformable laminated beams. They introduced a shear force at the crack tip, Q_C, but neglected the bending moment, M_C (Fig. 6c). Their expressions for the modal contributions are:

$$G_{\mathrm{I}}^{\mathrm{Wang,Qiao}} = \frac{1}{2B} \delta_Q Q_C^2 \quad \text{and} \quad G_{\mathrm{II}}^{\mathrm{Wang,Qiao}} = \frac{1}{2B} \delta_N N_C^2 \tag{20}$$

where, for orthotropic specimens, the coefficients take the following form:

$$\delta_Q = \frac{6}{5 G_{xz} B} \left(\frac{1}{H_1} + \frac{1}{H_2} \right) \quad \text{and} \quad \delta_N = \frac{4}{E_x B} \left(\frac{1}{H_1} + \frac{1}{H_2} \right) \tag{21}$$

According to Eqs. (20) and (21), shear forces and shear deformation contribute only to mode I.
Valvo [24] extended Williams' method from homogeneous beams to general laminated beams. He determined the modal contributions to G based on a modified virtual crack closure technique. By considering all the three stress resultants – N_C, Q_C, and M_C – at the crack tip (Fig. 6d), he obtained:

$$G_{\mathrm{I}}^{\mathrm{Valvo}}=\frac{1}{2B}\left(\frac{f_{uN}f_{\phi M}-f_{uM}f_{\phi N}}{f_{uN}}M_C^2+f_{wQ}Q_C^2\right)\quad\text{and}\quad G_{\mathrm{II}}^{\mathrm{Valvo}}=\frac{1}{2B}\frac{1}{f_{uN}}(f_{uN}N_C+f_{uM}M_C)^2 \tag{22}$$

where, for orthotropic specimens,

$$f_{uN}=\frac{4}{E_xB}\left(\frac{1}{H_1}+\frac{1}{H_2}\right),\quad f_{uM}=f_{\phi N}=\frac{6}{E_xB}\left(\frac{1}{H_1^2}-\frac{1}{H_2^2}\right),\quad f_{wQ}=\frac{6}{5G_{xz}B}\left(\frac{1}{H_1}+\frac{1}{H_2}\right),\quad\text{and}$$
$$f_{\phi M}=\frac{12}{E_xB}\left(\frac{1}{H_1^3}+\frac{1}{H_2^3}\right). \tag{23}$$

Comparison of Eqs. (22) and (23) with (20) and (21) shows that Valvo's method [24] reduces to Wang and Qiao's method [20], if the crack-tip bending moment, M_C, is disregarded. In general, however, M_C gives a contribution to both modes I and II. Instead, shear forces and shear deformation contribute only to mode I.

By substituting Eqs. (23) into (22) and expressing the crack-tip forces in terms of the internal forces on the delaminated sublaminates, the expressions for the modal contributions to the energy release rate become

$$G_{\mathrm{I}}^{\mathrm{Valvo}}=\frac{3}{8B^2E_x}(H_1-H_2)^2\frac{H_1H_2}{H^3}\left(\frac{N_1}{H_1}-\frac{N_2}{H_2}\right)^2+\frac{3}{5B^2G_{xz}}\frac{H_1H_2}{H}\left(\frac{Q_1}{H_1}-\frac{Q_2}{H_2}\right)^2+$$
$$+\frac{3}{2B^2E_x}\frac{H_1H_2}{H^3}\left(\frac{3H_1+H_2}{H_1^2}M_1-\frac{H_1+3H_2}{H_2^2}M_2\right)^2\quad\text{and} \tag{24}$$
$$G_{\mathrm{II}}^{\mathrm{Valvo}}=\frac{1}{8B^2E_x}\frac{H_1H_2}{H}\left(\frac{N_1}{H_1}-\frac{N_2}{H_2}\right)^2+\frac{9}{2B^2E_x}\frac{H_1H_2}{H}\left(\frac{M_1}{H_1^2}+\frac{M_2}{H_2^2}\right)^2$$

According to Eqs. (24), axial forces may contribute also to mode I. This contribution – neglected by both Williams' [16] and Wang and Qiao's [20] methods – passes through the crack-tip bending moment, M_C, and depends on the contribution of axial forces on the moment balance on the laminate cross section [24].

Elasticity-theory models

As opposite to Williams' global method [16], Suo and Hutchinson [17] developed a local method based on the analysis of the singular stress field at the delamination crack tip. They analysed the problem of a semi-infinite crack between two homogeneous and isotropic elastic layers subjected to axial forces and bending moments. First, they computed the energy release rate based on simple beam theory. Then, within linear elastic fracture mechanics, they solved numerically a plane elasticity problem to obtain the mode I and II stress intensity factors, K_{I} and K_{II} [48]. Li et al. [19] extended the local method to include the effects of shear forces.

Andrews and Massabò [21] further extended the method to include the effects of root rotations. They computed the total energy release rate based on the *J*-integral and then determined the stress intensity factors. Their analytical expressions depend on numerical coefficients obtained through finite element analyses and given in a tabular form. If no axial forces and bending moment are present, but only shear forces, their expression for the energy release rate takes the form

$$G_{\mathrm{Shear}}^{\mathrm{Andrews,Massabò}}=\frac{1}{E_xB^2H_1}\left[f_{V_D}^2V_D^2+f_{V_S}^2V_S^2+\frac{2}{H_1}f_{V_D}f_{V_S}V_DV_S\cos\left(\gamma_{V_D}-\gamma_{V_S}\right)\right] \tag{25}$$

and the stress intensity factors can be written as

$$K_{\mathrm{I,Shear}}^{\mathrm{Andrews,Massabò}}=\frac{\lambda^{3/8}}{\sqrt{H_1}}\left(\frac{2}{1+\rho}\right)^{1/4}\left[f_{V_D}V_D\cos\left(\gamma_{V_D}+\omega\right)+f_{V_S}V_S\cos\left(\gamma_{V_S}+\omega\right)\right]\quad\text{and}$$
$$K_{\mathrm{II,Shear}}^{\mathrm{Andrews,Massabò}}=-\frac{\lambda^{1/8}}{\sqrt{H_1}}\left(\frac{2}{1+\rho}\right)^{1/4}\left[f_{V_D}V_D\cos\left(\gamma_{V_D}+\omega\right)+f_{V_S}V_S\cos\left(\gamma_{V_S}+\omega\right)\right] \tag{26}$$

where

$$V_S = Q_1 + Q_2, \quad V_D = -Q_2, \quad \lambda = \frac{E_z}{E_x}, \quad \text{and} \quad \rho = \frac{\sqrt{E_x E_z}}{2G_{zx}} - \nu_{xz}\sqrt{\lambda} \tag{27}$$

The expressions for the parameters f_{VD}, f_{VS}, γ_{VD}, γ_{VD}, and ω are given in the cited paper [21]. The modal contributions to the energy release rate can then be computed as follows:

$$G_{\mathrm{I}}^{\text{Andrews,Massabò}} = \frac{1}{E_x}\sqrt{\frac{1+\rho}{2}}\lambda^{-3/4}K_{\mathrm{I}}^2 \quad \text{and} \quad G_{\mathrm{II}}^{\text{Andrews,Massabò}} = \frac{1}{E_x}\sqrt{\frac{1+\rho}{2}}\lambda^{-1/4}K_{\mathrm{II}}^2 \tag{28}$$

Inspection of Eqs. (26)–(28) shows that, according to elasticity theory, shear forces and the material shear modulus will generally affect both modes I and II.

Elastic-interface models

Bruno and Greco [30] specifically addressed the influence of shear deformation on delamination in the setting of elastic-interface models. They considered a two-layer plate with an elastic interface consisting of normal and tangential distributed springs and obtained an analytical solution by treating the spring constants as penalty parameters approaching infinity. They concluded that, for symmetric delamination, shear forces influence only the mode I contribution. Instead, for asymmetric delamination, shear forces are expected to affect both fracture modes. Furthermore, they found an interaction between shear forces and normal stresses coming from axial forces and bending moments.

Qiao and Wang [31] determined an analytical solution for a bilayer beam with an elastic interface. They computed the energy release rate through the *J*-integral [48] and determined the mode-mixity angle via an adaptation of Suo and Hutchinson's method [17]. In general, they found an influence of shear forces and shear deformation on both fracture modes.

Wang et al. [46] compared several mixed-mode partition methods based on SBT and TBT with rigid and deformable interfaces. In general, they found that shear forces cause additional contributions to both modes I and II.

Liu et al. [37] gave a general solution for adhesively bonded joints, where the adherends are modelled as Timoshenko beams and the adhesive layer is represented as an elastic interface. The interface consists of a continuous distribution of linearly elastic springs with constants k_z and k_x, respectively acting in the normal and tangential directions with respect to the interface plane (Fig. 7). Their solution can be used also for the analysis of delamination in composite laminates, if the interface is interpreted as a conventional means to account for the laminate transverse deformability and not as representative of a physical layer of adhesive.

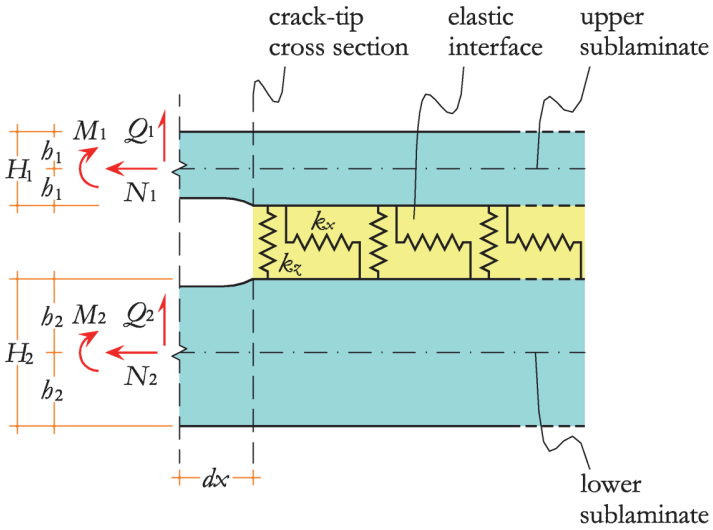

Figure 7: Elastic-interface model of a delaminated beam.

The modal contributions to the energy release rate can be expressed as [34]:

$$G_{\mathrm{I}}^{\mathrm{interface}} = \frac{1}{2}\frac{\sigma_0^2}{k_z} \quad \text{and} \quad G_{\mathrm{II}}^{\mathrm{interface}} = \frac{1}{2}\frac{\tau_0^2}{k_x} \tag{29}$$

where σ_0 and τ_0 respectively are the values of the normal and tangential interfacial stresses at the crack tip. For a homogeneous delaminated beam, such stresses turn out to have the following expressions [37]:

$$\sigma_0 = \sum_{i=1}^{4} f_i \quad \text{and} \quad \tau_0 = \sum_{i=5}^{7} f_i \tag{30}$$

for symmetric delamination, i.e. when $H_1 = H_2$, and

$$\sigma_0 = \sum_{i=1}^{6} g_i \quad \text{and} \quad \tau_0 = k_x \beta_0 \sum_{i=1}^{6} \frac{g_i}{\mu_i\left(\mu_i^2 - \alpha_3\right)} + g_7 \tag{31}$$

for general asymmetric delamination. In Eqs. (30) and (31), $f_1, f_2, \ldots, f_7$ and $g_1, g_2, \ldots, g_7$ are integration constants depending on the problem boundary conditions; furthermore,

$$\beta_0 = \frac{6}{E_x}\left(\frac{1}{H_1^2} - \frac{1}{H_2^2}\right) \quad \text{and} \quad \alpha_3 = \frac{4k_x}{E_x}\left(\frac{1}{H_1} + \frac{1}{H_2}\right) \tag{32}$$

are problem parameters, while $\mu_1, \mu_2, \ldots, \mu_6$ are the roots of the characteristic equation of the differential problem for the interfacial stresses [37].

Inspection of Eqs. (29) and (30) shows that, for symmetric delamination, it is possible to separate fracture modes, i.e. to give suitable boundary conditions producing $f_1 = f_2 = f_3 = f_4 = 0$, hence $G_{\mathrm{I}} = 0$ (pure mode II), or $f_5 = f_6 = f_7 = 0$, hence $G_{\mathrm{II}} = 0$ (pure mode I). In such cases, the analytical solution reported in Ref. [37] also shows that the sublaminate shear stiffnesses influence only the mode I contribution to the energy release rate. Instead, for asymmetric delamination, pure fracture modes cannot be obtained in general, since the normal and tangential stress components given by Eqs. (31) depend on the same integration constants, $g_1, g_2, \ldots, g_6$ (the last constant, g_7, corresponds to the Jourawski shear stress occurring in a unbroken laminate and therefore is irrelevant in fracture problems). Hence, for asymmetric delamination, mixed-mode fracture conditions are generally present. In this case, both the mode I and II contributions to G depend on shear deformation and shear forces.

Numerical example

To complete the above discussion with some quantitative results, a comparison will be made between the predictions for G_{I} and G_{II} stemming from (i) the rigid-connection model [24], (ii) the elastic-interface model [37], and (iii) the local method in the version by Andrews and Massabò [21]. The latter can be used for reference as it represents an exact solution obtained within the theory of elasticity.

For illustration, a homogeneous and orthotropic laminate is considered with cross-section sizes $B = 25$ mm and $H = 4$ mm and elastic moduli $E_x = 100$ GPa, $E_z = 10$ GPa, $G_{zx} = 5$ GPa, and $\nu_{xz} = 0.3$. Such properties are intended to be representative of a typical laminated specimen used in delamination toughness tests.

A beam segment at the delamination crack-tip is considered (Fig. 8a), subjected to shear forces Q_1 and Q_2 on the delaminated sublaminates and $Q_3 = Q_1 + Q_2$ on the unbroken part. To investigate all possible load conditions, the acting forces are decomposed into the sum of a symmetric system (Fig. 8b) and an antisymmetric system (Fig. 8c) with

$$Q_s = \frac{Q_1 - Q_2}{2} \quad \text{and} \quad Q_a = \frac{Q_1 + Q_2}{2} \tag{33}$$

With the above assumptions, for symmetric delamination, the symmetric and antisymmetric parts of the acting forces give rise to pure fracture modes I and II, respectively. But, if the delamination is not placed on the mid-plane, mixed-mode fracture conditions are expected.

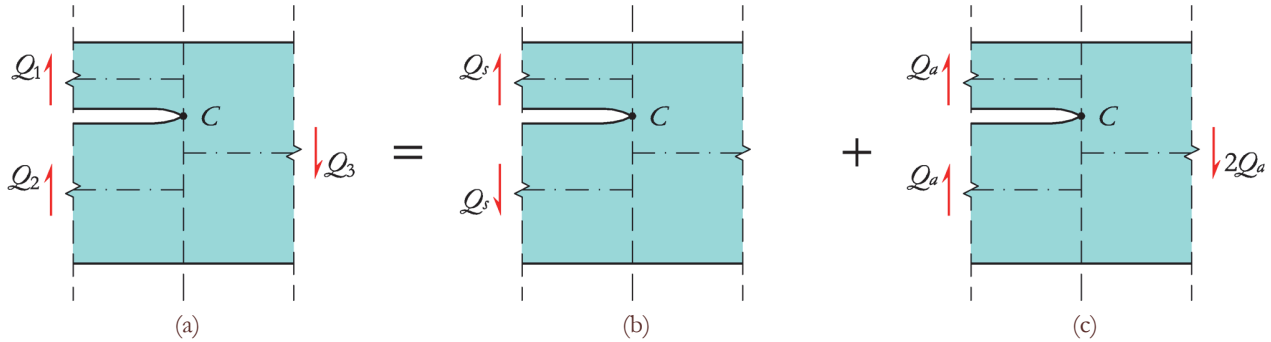

Figure 8: Decomposition of (a) the shear forces acting on a crack-tip segment into (b) symmetric and (c) antisymmetric systems.

Fig. 9 shows the mode I and II contributions to the energy release rate produced by two symmetric shear forces of intensity Q_s = 100 N applied at the crack tip, as functions of the sublaminate thickness ratio, $\eta = H_1/H_2$. Without loss of generality, attention is restricted to the case $H_1 \le H_2$, corresponding to $\eta \in [0,1]$. The limits $\eta \to 0$ and $\eta \to 1$ respectively correspond to thin-film debonding and symmetric delamination. Continuous red lines represent the predictions of the rigid-connection model [24] as computed from Eqs. (24). Dashed orange lines correspond to the elastic-interface model [37], as per Eqs. (29), for four increasing values (1, 10, 100, and 1000) of the dimensionless elastic-interface constants, $\mu_x = k_x H / G_{\tilde{x}\tilde{x}}$ and $\mu_{\tilde{z}} = k_{\tilde{z}} H / E_{\tilde{z}}$. Lastly, dotted blue lines correspond to the local method [21], as per Eqs. (28).

For the mode I contribution (Fig. 9a), all compared methods predict similar qualitative trends. The predictions of the elastic-interface model approach those of the rigid-connection model as the values of the elastic-interface constants increase. For $\mu_x = \mu_{\tilde{z}} \cong 10$, corresponding to $k_x = 12500$ N/mm^3 and $k_{\tilde{z}} = 25000$ N/mm^3, there is good matching between the elastic-interface model and the local method.

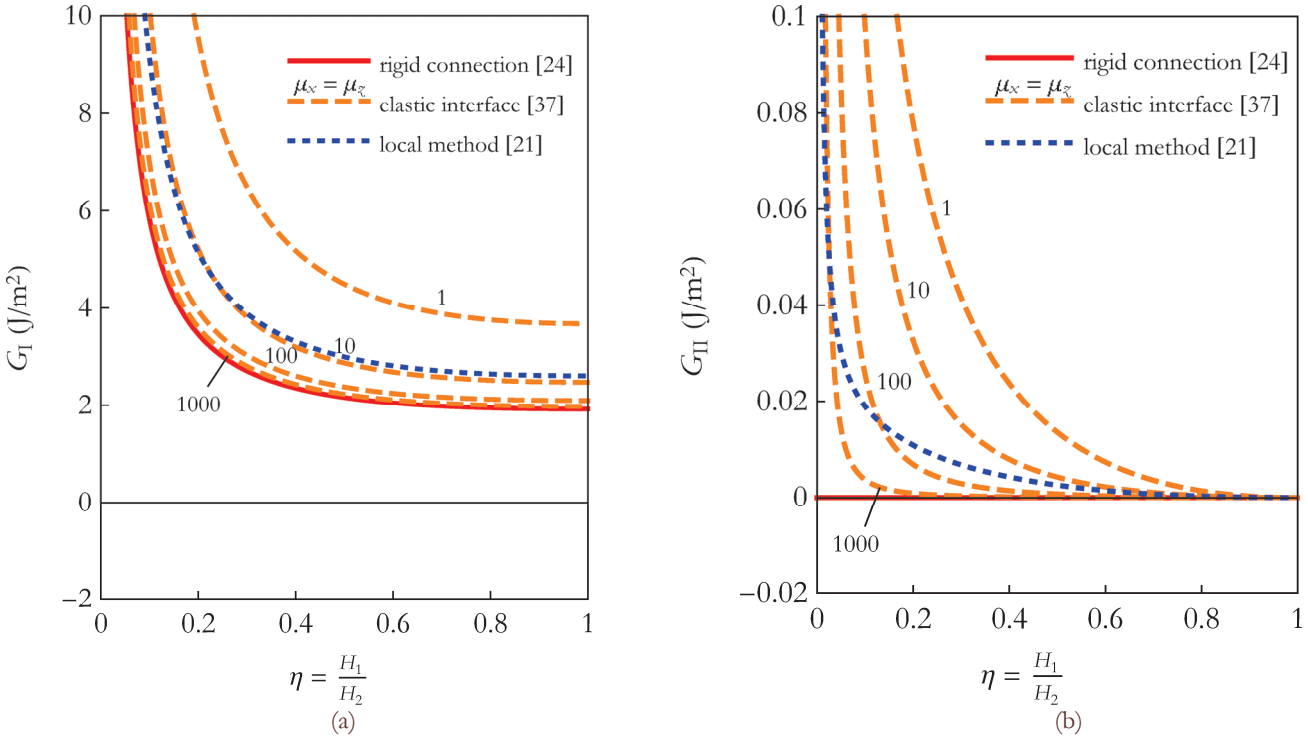

Figure 9: (a) Mode I and (b) mode II contributions to the energy release rate due to symmetric shear forces.

For the mode II contribution (Fig. 9b), the rigid-connection model predicts a null value over the whole range of thickness ratios. Instead, the elastic-interface model and local method predict non-zero mode II contributions. However, the computed G_{II} values turn out to be two orders of magnitude lower than the corresponding G_I values, as can be noticed

from the different scales on the ordinate axes. Thus, it can be concluded that the application of symmetric shear forces produces prevailing mode I fracture conditions, regardless of the asymmetry in the position of the delamination crack. For symmetric delamination ($\eta \to 1$), all compared methods predict $G_{\mathrm{II}} = 0$, i.e. pure mode I fracture conditions.

Fig. 10 shows the mode I and II contributions to the energy release rate produced by two antisymmetric shear forces of intensity $Q_a = 100$ N applied at the crack tip, as functions of the sublaminate thickness ratio. The same graphical conventions of Fig. 9 are used to denote the predictions of the rigid-connection model [24], the elastic-interface model [37], and the local method [21]. Also, similar comments apply.

For the mode I contribution (Fig. 10a), the elastic-interface model approaches the rigid-connection model as μ_x and μ_z increase. Again, the predictions of the elastic-interface model match closely those of the local method for $\mu_x = \mu_z \cong 10$.

For the mode II contribution (Fig. 10b), the rigid-connection model predicts a null value over the whole range of thickness ratios. Instead, the elastic-interface model and local method predict non-zero mode II contributions. The computed G_{II} values are lower than the corresponding G_{I} values for smaller thickness ratios. Mixed-mode fracture conditions generally occur, with the mode II contribution increasing as η increases and G_{I} correspondingly decreases. For symmetric delamination ($\eta \to 1$), all compared methods predict $G_{\mathrm{I}} = 0$, i.e. pure mode II fracture conditions.

Lastly, it should be noticed that the above numerical results correspond to the application of only shear forces at the crack tip. In general, however, bending moments and axial forces will be present as well. Indeed, their contributions to the energy release rate may be quite larger than that due to shear. However, a quantitative assessment of those effects requires referring to specific cases in terms of geometry, loads, boundary conditions, etc. This assessment is not pursued within this paper, as focus here is on shear forces and their effects on mode II delamination.

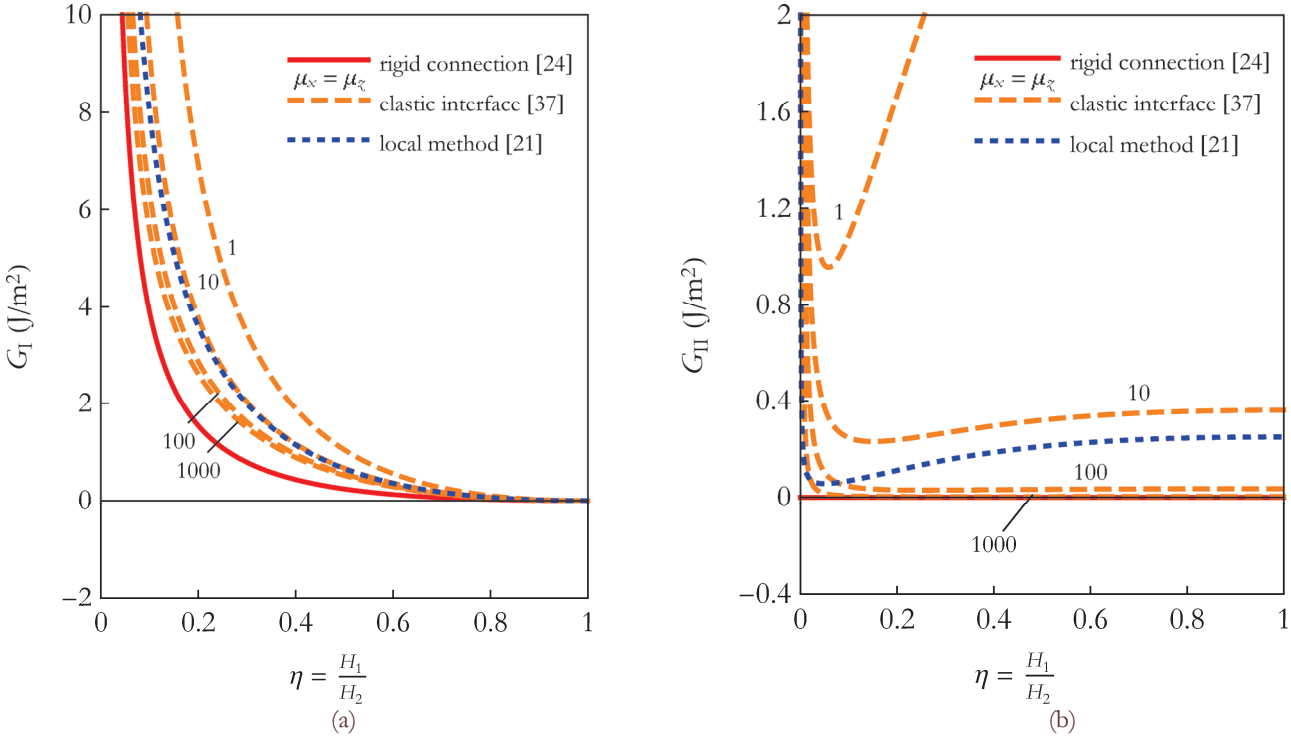

Figure 10: (a) Mode I and (b) mode II contributions to the energy release rate due to antisymmetric shear forces.

Conclusions

Shear deformation is relevant for composite materials because of their anisotropic elastic behaviour, regardless of the slenderness of beam-like structural elements. As such, shear deformation increases the compliance of laminated beams affected by delamination and, consequently, may influence the energy release rate associated to delamination growth. In this paper, the effects of shear deformation and shear forces on the mode II contribution to the energy release rate have been examined in the light of different structural theories and fracture mode partition methods of the literature.

First, attention has been devoted to the analysis of the ENF test as the prototype of symmetrically delaminated laminates subjected to pure mode II fracture conditions. Comparison of the available models reveals that shear deformation as accounted for at first order by the Timoshenko beam theory affects the specimen compliance, but not the mode II energy release rate. The shear-deformation correction terms given in Ref. [53] and used in much of the later literature turned out to be incorrect. Hence, their use for experimental test interpretation and comparison of models should be avoided in the future. Indeed, three-dimensional finite element analyses of the ENF test show a dependence of the energy release rate on the shear modulus of the material. This behaviour may be related to local deformation occurring at the delamination crack tip because of high stress concentration, e.g. strain in the laminate thickness direction, Poisson's effect, and root rotations. Such effects can be captured also with beam theory models, however based on higher-order shear-deformation theories or through the introduction of deformable interfaces connecting the delaminated sublaminates. Similar considerations hold in general for laminates with symmetric, i.e. mid-plane, delamination.

Next, a general delaminated beam has been considered with an arbitrarily located through-the-width delamination. In this case, mixed-mode fracture conditions generally occur and G_{II} is only a part of the total energy release rate. In the paper, several mixed-mode partition methods of the literature have been reviewed with specific attention on the effects of shear forces and shear deformation on G_{II}. Lastly, a quantitative comparison has been made between the predictions of the rigid-connection model [24], elastic-interface model [37], and local method [21] for a homogeneous and orthotropic laminate with shear forces applied at the crack tip. The results show a quite limited influence of the shear forces on the mode II contribution to the energy release rate, except for nearly symmetric delamination and antisymmetric shear forces.

For the sake of simplicity, in the paper, attention has been limited to homogeneous and orthotropic beams. Further studies will be necessary to extend the above considerations to more complex structural elements, such as bi-material and multidirectional laminated beams and plates.

REFERENCES

[1] Garg, A.C., (1988). Delamination-a damage mode in composite structures, Eng. Fract. Mech., 29, pp. 557–584. DOI: 10.1016/0013-7944(88)90181-6.

[2] Sela, N. and Ishai, O., (1989). Interlaminar fracture toughness and toughening of laminated composite materials: a review, Composites, 20, pp. 423–435. DOI: 10.1016/0010-4361(89)90211-5.

[3] Bolotin, V.V., (1996). Delaminations in composite structures: its origin, buckling, growth and stability, Compos. Part B-Eng., 27, pp. 129–145. DOI: 10.1016/1359-8368(95)00035-6.

[4] Tay, T.E., (2003). Characterization and analysis of delamination fracture in composites: An overview of developments from 1990 to 2001, Appl. Mech. Rev., 56 1–31. DOI: 10.1115/1.1504848.

[5] Senthil, K., Arockiarajan, A., Palaninathan, R., Santhosh, B., Usha, K.M., (2013). Defects in composite structures: Its effects and prediction methods – A comprehensive review, Compos. Struct., 106, pp. 139–149. DOI: 10.1016/j.compstruct.2013.06.008.

[6] Chatterjee, S.N. and Ramnath, V., (1988). Modeling laminated composite structures as assemblage of sublaminates, Int. J. Solids Struct., 24, pp. 439–458. DOI: 10.1016/0020-7683(88)90001-7.

[7] Reid, S.R., Zou, Z., Soden, P.D. and Li, S., (2001). Mode separation of energy release rate for delamination in composite laminates using sublaminates, Int. J. Solids Struct., 38, pp. 2597–2613. DOI: 10.1016/S0020-7683(00)00172-4.

[8] Jones, R.M., (1999). Mechanics of composite materials, second ed., Taylor & Francis, Philadelphia.

[9] Timoshenko, S.P., (1955).Strength of Materials, Vol. 1: Elementary Theory and Problems, third ed., D. Van Nostrand, New York.

[10] Timoshenko, S.P. and Woinowsky-Krieger, S., (1959). Theory of Plates and Shells, second ed., McGraw-Hill, New York.

[11] Reddy, J.N., (1984). A Simple Higher-Order Theory for Laminated Composite Plates, J. Appl. Mech., 51, pp. 745–752. DOI: 10.1115/1.3167719.

[12] Adim, B., Daouadji, T.H. and Rabahi, (2016). A simple higher order shear deformation theory for mechanical behavior of laminated composite plates, Int. J. Adv. Struct. Eng., 8, pp. 103–117. DOI: 10.1007/s40091-016-0109-x.

[13] Barbero, E.J. and Reddy, J.N., (1991). Modeling of delamination in composite laminates using a layer-wise plate theory, Int. J. Solids Struct., 28, pp. 373–388. DOI: 10.1016/0020-7683(91)90200-Y.

[14] Williams, T.O. and Addessio, F.L., (1997). A general theory for laminated plates with delaminations, Int. J. Solids Struct., 34, pp. 2003–2024. DOI: 10.1016/S0020-7683(96)00131-X.

[15] Pook, L.P., (1979). Approximate stress intensity factors obtained from simple plate bending theory, Eng. Fract. Mech., 12, pp. 505–522. DOI: 10.1016/0013-7944(79)90093-6.
[16] Williams, J.G., (1988). On the calculation of energy release rates for cracked laminates, Int. J. Fract., 36, pp. 101–119. DOI: 10.1007/BF00017790.
[17] Suo, Z. and Hutchinson, J.W., (1990). Interface crack between two elastic layers, Int. J. Fract., 43, pp. 1–18. DOI: 10.1007/BF00018123.
[18] Schapery, R.A. and Davidson, B.D., (1990). Prediction of energy release rate for mixed-mode delamination using classical plate theory, Appl. Mech. Rev., 43, pp. S281–S287. DOI: 10.1115/1.3120829.
[19] Li, S., Wang, J. and Thouless, M.D., (2004). The effects of shear on delamination in layered materials, J. Mech. Phys. Solids, 52, pp. 193–214. DOI: 10.1016/S0022-5096(03)00070-X.
[20] Wang, J. and Qiao, P., (2005). Mechanics of Bimaterial Interface: Shear Deformable Split Bilayer Beam Theory and Fracture, J. Appl. Mech., 72, pp. 674–682. DOI:10.1115/1.1978920.
[21] Andrews, M.G. and Massabò, R., (2007). The effects of shear and near tip deformations on energy release rate and mode mixity of edge-cracked orthotropic layers, Eng. Fract. Mech., 74, pp. 2700–2720. DOI: 10.1016/j.engfracmech.2007.01.013.
[22] Harvey, C.M. and Wang, S., (2012). Mixed-mode partition theories for one-dimensional delamination in laminated composite beams, Eng. Fract. Mech., 96, pp. 737–759. DOI: 10.1016/j.engfracmech.2012.10.001.
[23] Li, W., Cheng, G., Wang, D. and Wu, J., (2015). A mixed mode partition method for delaminated beam structure, Eng. Fract. Mech., 148, pp. 15–26. DOI: 10.1016/j.engfracmech.2015.09.005.
[24] Valvo, P.S., (2016). On the calculation of energy release rate and mode mixity in delaminated laminated beams, Eng. Fract. Mech., 165, pp. 114–139. DOI: 10.1016/j.engfracmech.2016.08.010.
[25] Kanninen, M.F., (1973). An augmented double cantilever beam model for studying crack propagation and arrest, Int. J. Fract., 9, pp. 83–92. DOI: 10.1007/BF00035958.
[26] Allix, O. and Ladeveze, P., (1992). Interlaminar interface modelling for the prediction of delamination, Compos. Struct., 22, pp. 235–242. DOI: 10.1016/0263-8223(92)90060-P.
[27] Corigliano, A., (1993). Formulation, identification and use of interface models in the numerical analysis of composite delamination, Int. J. Solids Struct., 30, pp. 2779–2811. DOI: 10.1016/0020-7683(93)90154-Y.
[28] Point, N. and Sacco, E., (1996). A delamination model for laminated composites, Int. J. Solids Struct., 33, pp. 483–509. DOI: 10.1016/0020-7683(95)00043-A.
[29] Bruno, D., Greco, F., (2001). Mixed mode delamination in plates: A refined approach, Int. J. Solids Struct., 38, pp. 9149–9177. DOI: 10.1016/S0020-7683(01)00179-2.
[30] Bruno, D. and Greco, F., (2001). Delamination in composite plates: influence of shear deformability on interfacial debonding, Cement Concrete Comp., 23, pp. 33–45. DOI: 10.1016/S0958-9465(00)00068-8.
[31] Qiao, P. and Wang, J., (2004). Mechanics and fracture of crack tip deformable bi-material interface, Int. J. Solids Struct., 41, pp. 7423–7444. DOI: 10.1016/j.ijsolstr.2004.06.006.
[32] Bennati, S. and Valvo, P.S., (2006). Delamination growth in composite plates under compressive fatigue loads, Compos. Sci. Technol., 66, pp. 248–254. DOI: 10.1016/j.compscitech.2005.04.035.
[33] Szekrényes, A., (2007). Improved analysis of unidirectional composite delamination specimens, Mech. Mater., 39, pp. 953–974. DOI: 10.1016/j.mechmat.2007.04.002.
[34] Bennati, S., Colleluori, M., Corigliano, D. and Valvo, P.S., (2009). An enhanced beam-theory model of the asymmetric double cantilever beam (ADCB) test for composite laminates, Compos. Sci. Technol., 69, pp. 1735–1745. DOI: 10.1016/j.compscitech.2009.01.019.
[35] Bennati, S., Fisicaro, P. and Valvo, P.S., (2013). An enhanced beam-theory model of the mixed-mode bending (MMB) test – Part I: Literature review and mechanical model, Meccanica, 48, pp. 443–462. DOI: 10.1007/s11012-012-9686-3.
[36] Bennati, S., Fisicaro, P. and Valvo, P.S., (2013). An enhanced beam-theory model of the mixed-mode bending (MMB) test – Part II: applications and results, Meccanica, 48, pp. 465–484. DOI: 10.1007/s11012-012-9682-7.
[37] Liu, Z., Huang, Y., Yin, Z., Bennati, S. and Valvo, P.S., (2014). A general solution for the two-dimensional stress analysis of balanced and unbalanced adhesively bonded joints, Int. J. Adhes. Adhes., 54, pp. 112–123. DOI: 10.1016/j.ijsolstr.2013.06.021.
[38] Dimitri, R., Tornabene, F. and Zavarise, G., (2018). Analytical and numerical modeling of the mixed-mode delamination process for composite moment-loaded double cantilever beams, Compos. Struct., 187, pp. 535–553. DOI: 10.1016/j.compstruct.2017.11.039.
[39] Borg, R., Nilsson, L. and Simonsson, K., (2001). Simulation of delamination in fiber composites with a discrete cohesive failure model, Compos. Sci. Technol. 61, pp. 667–677. DOI: 10.1016/S0266-3538(00)00245-1.

[40] Camanho, P.P., Dávila, C.G. and de Moura, M.F., (2003). Numerical simulation of mixed-mode progressive delamination in composite materials, J. Compos. Mater., 37, pp. 1415–1438. DOI: 10.1177/0021998303034505.
[41] Yang, Q. and Cox, B., (2005). Cohesive models for damage evolution in laminated composites, Int. J. Fract., 133, pp. 107–137. DOI: 10.1007/s10704-005-4729-6.
[42] Parmigiani, J.P. and Thouless, M.D., (2007). The effects of cohesive strength and toughness on mixed-mode delamination of beam-like geometries, Eng. Fract. Mech., 74, pp. 2675–2699. DOI: 10.1016/j.engfracmech.2007.02.005.
[43] Turon, A., Dávila, C.G., Camanho, P.P. and Costa, J., (2007). An engineering solution for mesh size effects in the simulation of delamination using cohesive zone models, Eng. Fract. Mech., 74, pp. 1665–1682. DOI: 10.1016/j.engfracmech.2006.08.025.
[44] Harper, P.W. and Hallett, S.R., (2008). Cohesive zone length in numerical simulations of composite delamination, Eng. Fract. Mech., 75, pp. 4774–4792. DOI: 10.1016/j.engfracmech.2008.06.004.
[45] Sørensen, B.F. and Jacobsen T.K., (2009). Characterizing delamination of fibre composites by mixed mode cohesive laws, Compos. Sci. Technol., 69, pp. 445–456. DOI: 10.1016/j.compscitech.2008.11.025.
[46] Wang, S., Harvey, C.M. and Guan, L. (2013). Partition of mixed modes in layered isotropic double cantilever beams with non-rigid cohesive interfaces, Eng. Fract. Mech., 111, pp. 1–25. DOI: 10.1016/j.engfracmech.2013.09.005.
[47] Dimitri, R., Trullo, M., De Lorenzis, L. and Zavarise, G., (2015). Coupled cohesive zone models for mixed-mode fracture: A comparative study, Eng. Fract. Mech., 148, pp. 145–179. DOI: 10.1016/j.engfracmech.2015.09.029.
[48] Friedrich, K. (Ed.), (1989). Application of Fracture Mechanics to Composite Materials, Elsevier, Amsterdam.
[49] Hutchinson, J.W. and Suo, Z., (1991). Mixed mode cracking in layered materials, Adv. Appl. Mech., 29, pp. 63–191. DOI: 10.1016/S0065-2156(08)70164-9-
[50] Carlsson, L.A., Adams, D.F. and Pipes, R.B., (2014). Experimental Characterization of Advanced Composite Materials, fourth ed., CRC Press, Boca Raton.
[51] ASTM D7905/D7905M-14, Standard Test Method for Determination of the Mode II Interlaminar Fracture Toughness of Unidirectional Fiber-Reinforced Polymer Matrix Composites, ASTM International, West Conshohocken, (2014). DOI: 10.1520/D7905_D7905M-14.
[52] Russell, A.J. and Street, K.N., (1985). Moisture and temperature effects on the mixed-mode delamination fracture of unidirectional graphite/epoxy, in: W.S. Johnson (Ed.), Delamination and Debonding of Materials, ASTM STP 876, ASTM, Philadelphia, pp. 349–370. DOI: 10.1520/STP36314S.
[53] Carlsson, L.A., Gillespie Jr, J.W. and Pipes, R.B., (1986). On the Analysis and Design of the End Notched Flexure (ENF) Specimen for Mode II Testing, J. Compos. Mat., 20, pp. 594–604. DOI: 10.1177/002199838602000606.
[54] Gillespie Jr, J.M., Carlsson, L.A. and Pipes, R.B., (1986). Finite element analysis of the end notched flexure specimen for measuring mode II fracture toughness, Compos. Sci. Technol., 27, pp. 177–197. DOI: 10.1016/0266-3538(86)90031-X.
[55] Whitney, J.M., (1990). Analysis of Interlaminar Mode II Bending Specimens Using a Higher Order Beam Theory, J. Reinf. Plast. Compos., 9, pp. 522–536. DOI: 10.1177/073168449000900601.
[56] Chatterjee, S.N., (1991). Analysis of Test Specimens for Interlaminar Mode II Fracture Toughness, Part 1. Elastic Laminates, J. Compos. Mater., 25, pp. 470–493. DOI: 10.1177/002199839102500501.
[57] Wang, Y. and Williams, J.G., (1992). Corrections for mode II fracture toughness specimens of composites materials, Compos. Sci. Technol., 43, pp. 251–256. DOI: 10.1016/0266-3538(92)90096-L.
[58] Corleto, C.R. and Hogan, H.A., (1995). Energy Release Rates for the ENF Specimen Using a Beam on an Elastic Foundation, J. Compos. Mat., 29, pp. 1420–1436. DOI: 10.1177/002199839502901101.
[59] Ozdil, F., Carlsson, L.A. and Davies, P., (1998). Beam analysis of angle-ply laminate end-notched flexure specimens, Compos. Sci. Technol., 58, pp. 1929–1938. DOI: 10.1016/S0266-3538(98)00018-9.
[60] Ding, W. and Kortschot, M.T., (1999). A simplified beam analysis of the end notched flexure mode II delamination specimen, Compos. Struct., 45, pp. 271–278. DOI: 10.1016/S0263-8223(99)00030-6.
[61] Pavan Kumar, D.V.T.G. and Raghu Prasad, B.K., (2003). Higher-Order Beam Theories for Mode II Fracture of Unidirectional Composites, J. Appl. Mech., 70, pp. 840–852. DOI: 10.1115/1.1607357.
[62] Wang, J. and Qiao, P., (2004). Novel beam analysis of end notched flexure specimen for mode-II fracture, Eng. Fract. Mech., 71, pp. 219–231. DOI: 10.1016/S0013-7944(03)00096-1.
[63] Silva, M.A.L., de Moura, M.F.S.F. and Morais, J.J.L., (2006). Numerical analysis of the ENF test for mode II wood fracture, Compos. Part A-Appl. S., 37, pp. 1334–1344. DOI: 10.1016/j.compositesa.2005.08.014.
[64] Fan, C., Ben Jar, P.-Y. and Cheng, J.-J.R., (2007). Revisit the analysis of end-notched-flexure (ENF) specimen, Compos. Sci. Technol., 66, pp. 1497–1498. DOI: 10.1016/j.compscitech.2006.01.016.

[65] Raghu Prasad, B.K. and Pavan Kumar, D.V.T.G., (2008). Analysis of composite ENF specimen using higher order beam theories, Thin Wall. Struct., 46, pp. 676–688. DOI: 10.1016/j.tws.2007.11.004.
[66] Reeder, J.R. and Crews Jr, J.H., (1992). Redesign of the mixed-mode bending delamination test to reduce nonlinear effects, J. Compos. Tech. Res., 14, pp. 12–19. DOI: 10.1520/CTR10078J.
[67] Ducept, F., Davies, P. and Gamby, D., (1997). An experimental study to validate tests used to determine mixed mode failure criteria of glass/epoxy composites, Compos. Part A-Appl. S., 28, pp. 719–729. DOI: 10.1016/S1359-835X(97)00012-2.
[68] Beghini, M., Bertini, L. and Forte, P., (2006). Experimental investigation on the influence of crack front to fiber orientation on fatigue delamination growth rate under mode II, Compos. Sci. Technol., 66, pp. 240–247. DOI: 10.1016/j.compscitech.2005.04.033.
[69] Davies, P., Sims, G.D., Blackman, B.R.K., Brunner, A.J., Kageyama, K., Hojo, M., Tanaka, K., Murri, G., Rousseau, C., Gieseke, B. and Martin, R.H., (1999). Comparison of test configurations for determination of mode II interlaminar fracture toughness results from international collaborative test programme, Plast. Rubber Compos., 28, pp. 432–437. DOI: 10.1179/146580199101540600.
[70] Agrawal, A. and Ben Jar, P.-Y., (2003). Analysis of specimen thickness effect on interlaminar fracture toughness of fibre composites using finite element models, Compos. Sci. Technol., 63, pp. 1393–1402. DOI: 10.1016/S0266-3538(03)00088-5.
[71] Theotokoglou, E.E. and Vrettos, C.D., (2006). A finite element analysis of angle-ply laminate end-notched flexure specimens, Compos. Struct., 73, pp. 370–379. DOI: 10.1016/j.compstruct.2005.02.010.
[72] Irwin, G.R. and Kies, J.A., (1954). Critical energy release rate analysis of fracture strength. Weld. J. Res. Suppl., 33, pp. 193–198.
[73] van der Meer, F.P. and Sluys, L.J., (2009). A phantom node formulation with mixed mode cohesive law for splitting in laminates, Int. J. Fract., 158, pp. 107–124. DOI: 10.1007/s10704-009-9344-5.
[74] Thouless, M.D., (2009). The effects of transverse shear on the delamination of edge-notch flexure and 3-point bend geometries, Compos. Part B-Eng., 40, pp. 305–312. DOI: 10.1016/j.compositesb.2009.01.005.
[75] Wang, F., Shao, Z. and Wu, Y., (2013). Mode II interlaminar fracture properties of Moso bamboo, Compos. Part B-Eng., 44, pp. 242–247. DOI: 10.1016/j.compositesb.2012.05.035.
[76] Liu, P.F., Gu, Z.P. and Peng, X.Q., (2016). A nonlinear cohesive/friction coupled model for shear induced delamination of adhesive composite joint, Int. J. Fract., 199, pp. 135–156. DOI: 10.1007/s10704-016-0100-3.
[77] Li, Y., Stapleton, S.E., Simon, J.-W. and Reese, S., (2016). Experimental and Numerical Study of Paperboard Interface Properties, Exp. Mech., 56, pp. 1477–1488. DOI: 10.1007/s11340-016-0184-8.
[78] Valvo, P.S., (2008). Does shear deformability influence the mode II delamination of laminated beams?, in: J. Pokluda, P. Lukáš, P. Šandera, I. Dlouhý (Eds.), 17th European Conference on Fracture: Multilevel approach to fracture of materials, components and structures, European Structural Integrity Society (ESIS), Brno, pp. 1470–1477.
[79] Sundararaman, V. and Davidson, B., (1998). An unsymmetric end-notched flexure test for interfacial fracture toughness determination, Eng. Fract. Mech., 60, pp. 361–377. DOI: 10.1016/S0013-7944(98)00017-4.
[80] Yang, Z. and Sun, C.T., (2000). Interlaminar Fracture Toughness of a Graphite/Epoxy Multidirectional Composite, J. Eng. Mater. Technol., 122, pp. 428–433. DOI: 10.1115/1.1289027.
[81] Samborski, S., (2017). Analysis of the end-notched flexure test configuration applicability for mechanically coupled fiber reinforced composite laminates, Compos. Struct., 163, pp. 342-349. DOI: 10.1016/j.compstruct.2016.12.051.
[82] Bieniaś, J., Dadej, K. and Surowska, B., (2017). Interlaminar fracture toughness of glass and carbon reinforced multidirectional fiber metal laminates, Eng. Fract. Mech., 175, pp. 127-145. DOI: 10.1016/j.engfracmech.2017.02.007.
[83] ASTM D6671/D6671M-13e1, Standard Test Method for Mixed Mode I-Mode II Interlaminar Fracture Toughness of Unidirectional Fiber Reinforced Polymer Matrix Composites, ASTM International, West Conshohocken, (2013). DOI: 10.1520/D6671_D6671M-13E01.